Geomechanics and Engineering, *Vol. 19, No. 4 (2019) 329-342*
DOI: https://doi.org/10.12989/gae.2019.19.4.329

Behavior of sand columns reinforced by vertical geotextile encasement and horizontal geotextile layers

Mohammad Shamsi[1a], Ali Ghanbari[1b] and Javad Nazariafshar[*2]

[1]*Department of Civil Engineering, Kharazmi University of Tehran, No.49 Mofattah Ave, Tehran, Iran*
[2]*Department of Civil Engineering, Shahr-e-Qods Branch, Islamic Azad University, Tehran, Iran*

(Received May 3, 2019, Revised October 24, 2019, Accepted November 8, 2019)

Abstract. In this paper, the effect of a group of sand columns in the loose soil bed using triaxial tests was studied. To investigate the effect of geotextile reinforcement type on the bearing capacity of these sand columns, Vertical encased sand columns (VESCs) and horizontally reinforced sand columns (HRSCs) were used. Number of sixteen independent triaxial tests and finite element simulation were performed on specimens with a diameter of 100 mm and a height of 200 mm. Specimens were reinforced by either a single sand column or three sand columns with the same area replacement ratio (16%) to evaluate the Influence of the column arrangement. Effect the number of sand columns, the length of vertical encasement and the number of horizontal reinforcing layers were investigated, in terms of bearing capacity improvement and economy. The results indicated that the ultimate bearing capacity of the samples with three ordinary sand columns (OSCs) is eventually about 11% more than samples with an OSC. Also, comparison of the column reinforcing modes showed that four horizontal layers of geotextile achieved similar performance to a vertical encasement geotextile at the 50% of the column height, from the viewpoint of strength improvement, while from the viewpoint of economy, the geotextile needed for encasing the single column is around 2.5 times of the geotextile required for four layers.

Keywords: geosynthetics; stone columns; loose soil bed; geotextile encasement; horizontal geotextile layers

1. Introduction

Ground improvement using stone columns is well suited for the improvement of soft or loose soils such as silty sand, silts, and clays (Keykhosropur and Imam 2012, Zhang *et al.* 2012, Kadhim *et al.* 2018). Stone columns are successfully used to support the buildings and embankments, to improve the bearing capacity of raft foundations, to increase the stability of slopes and to reduce the liquefaction potential of loose sands (Barksdale and Bachus 1983, Deb and Majee 2014, Gu *et al.* 2017, McGuire *et al.* 2019). Despite the advantages of the stone column in improving the behavior of the soil bed, this technique may not be effective for the improvement of soft or loose soils. In the low strength soils, after the installation of the stone columns and loading, due to the lack of sufficient lateral confinement for the columns, the granular columns fail and their efficiency decreases. In order to prevent the failure of the stone column and provide lateral confinement to increase the bearing capacity of the low strength soils bed, the stone columns are usually reinforced by encasement geosynthetics (wrapping the column with a geosynthetic) or horizontal disks of geosynthetics (Najjar *et al.* 2010, Ali *et al.* 2012, 2014, Hosseinpour *et al.* 2014, Ghazavi *et al.* 2018). In recent years, several laboratory triaxial tests have been conducted to evaluate the performance of sand columns (OSCs, HRSCs or VESCs) in the triaxial specimens (Malarvizhi and Ilamparuthi 2007, Black *et al.* 2007a, b, Madhavi and Murthy 2007, Wu and Hong 2008, 2009, Black *et al.* 2011, Hong and Wu 2013, Nguyen *et al.* 2013, Frikha *et al.* 2014, Miranda and Costa 2016). As stone columns are generally used beneath uniformly loaded areas such as embankments, the triaxial test can adequately capture the confinement and group interaction of these applications, in contrast to the common method of testing isolated columns (Gniel and Bouazza 2009). The unit cell approach was expected to adequately represent column behavior beneath the center of a widely loaded area such as an embankment. The researchers who resorted to triaxial testing specimens reinforced by sand columns and investigated qualitatively application of the laboratory tests data to field behavior include the work reported in Juran and Guermazi (1988), Sivakumar *et al.* (2004), McKelvey *et al.* (2004), Gniel and Bouazza (2009), Najjar *et al.* (2010), Sivakumar *et al.* (2011), and Frikha *et al.* (2015). It is recognized that the results of these studies and columns embedded in the field somewhat differ in load and boundary conditions, although understanding the reinforcing mechanism and the factors essential to the column behavior contributes significantly to the advancement of embedded column studies. In spite of many studies on the behavior of the granular columns in saturated clay beds, only a very limited number of laboratory studies have been carried out on stone/sand

∗Corresponding author, Assistant Professor
E-mail: j.nazariafshar@qodsiau.ac.ir
[a]Ph.D. Student
E-mail: mohamad.shamsi70@gmail.com
[b]Professor
E-mail: ghanbari@khu.ac.ir

http://www.techno-press.org/?journal=gae&subpage=7
ISSN: 2005-307X (Print), 2092-6219 (Online)

columns in the low strength grained soil bed (Kadhim *et al.* 2018, Cengiz *et al.* 2019). Sivakumar *et al.* (2004) carried out a series test using triaxial apparatus in order to evaluate the behavior of clay samples with a diameter of 100 and a height of 200 mm installed with a VESC of 32 mm diameter. The results concluded that geogrid reinforcement produced significant increases in load-carrying capacity. Najjar *et al.* (2010) performed CU triaxial tests on clay samples with a single VESC for area replacement ratios of 7.9% and 17.8%. The results demonstrated that encased columns improved the apparent cohesion of the composite, particularly for small area replacement ratios. Hosseinpour *et al.* (2014) investigated the effect of the stone columns reinforced by vertical geotextile encasement and horizontal geotextile disks at different intervals by means of the unit cell finite element analyses. They showed that the optimum interval between horizontal geotextile disks to achieve the same performance as encased stone columns is dependent on the geotextile stiffness and the reinforced length of the column. Frikha *et al.* (2015) used CU triaxial tests to study the behavior of clay samples with a diameter of 70 mm and a height of 140 mm containing one, three, and four OSCs in the same area replacement ratio. Results indicated an increase in the effective friction angle with the increase in the number of columns. Fattah *et al.* (2016) investigated the behavior of embankment models resting on soft soil reinforced by a group of encased stone columns with a rectangular pattern. They reported that when models reinforced by stone columns at S = 2.5D, A higher improvement in bearing capacity was achieved at any embankment height, where D is the column diameter; and S is the spacing between columns.

The effect of geotextile encasement in the previous works have been confirmed through various numerical studies or laboratory tests; however, each of these cases focuses on only encasing the granular columns over the full column length, and hence only a few studies (Gniel and Bouazza 2009, Demir and Sarici 2017) into the influence of partially encased column (encasing the columns at the zone that maximum bulging occurs) appear. Also in the case of reinforced stone columns, very limited studies (Nazariafshar and Ghazavi 2014) exist on the use of geotextile layers and encasement simultaneously. Furthermore, most of these studies are comparing the geotextiles disks and encasement in terms of bearing capacity improvement, and very little information is available on this comparison from the viewpoint of economy. The above literature indicates that there is a lack of research into the behavior of the unreinforced and reinforced group of sand columns with different patterns in loose soil bed. Therefore, in this research, small-scale laboratory tests and numerical simulations were performed on samples of 100 mm diameter and 200 mm in height, in order to investigate the following factors:

1. Effect of a group of the granular columns in a loose soil bed
2. Comparison between geotextile encasement and horizontal disks, in terms of load bearing capacity improvement and economy
3. Effect of the number of granular columns installed in the specified area with the same area replacement ratio from an economic, executive, and improved shear strength.

2. Experimental procedure

2.1 Materials

In the current study, the Firoozkooh silica sand was used as sand column materials. Also, the natural soil (passing sieve No.10#) was used as surrounding loose soil bed that was obtained from the city center of Tehran at a depth of 1.5 to 2 m. A type of nonwoven geotextile was used to reinforcing the sand column with horizontal geotextile layers or vertical encasement. The value of the geotextile stiffness (J) was at the lower end of the J typically associated with full-scale geotextiles, which generally range between 50 kN/m and 2000 kN/m. The properties of the soils and geotextile have been listed in Tables 1 and 2. Particle size distribution for soils used in this study is shown in Fig. 1. Based on ASTM D 4767, for triaxial test samples, the largest aggregate size should not exceed one-sixth of the sample diameter. This condition is established according to the gradation curves.

Table 1 Mechanical properties of soil materials

Parameters	Value	
	Surrounding soil bed	Sand column
Specific gravity	2.55	2.63
Maximum dry unit weight (kN/m^3)	17.4[a]	17.5[b]
Minimum dry unit weight (kN/m^3)	12.1	14.8
Optimum moisture content (%)	16.8	----
Plastic limit (%)	22	----
Plasticity index (%)	10	----
Unified system classification	SW-SC	SP

a: ASTM D 1557 (Modified Proctor test), b: ASTM D4253 – 14 (Vibratory Table test)

Table 2 Mechanical properties of geotextile (produced by DuPont ™ Typar®)

Area weigh (gr/m^2)	Thickness (mm)	Strain at ultimate strength (%)	Ultimate tensile strength (kN/m)	Ultimate stress of geotextile, S_U (MPa)	geotextile stiffness (kN/m)
90	0.4	40	21	52.5	52

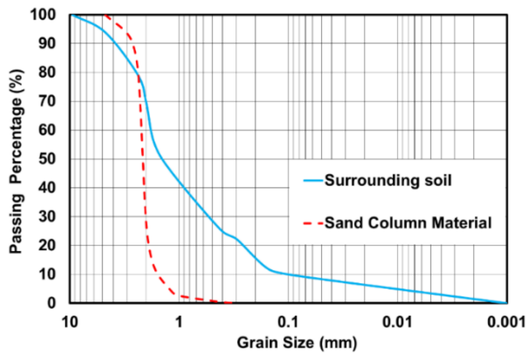

Fig. 1 Particle size distribution for surrounding loose soil bed and sand column material

Table 3 Summary of the testing program

Test series	Test number	Test Name	Test description	Number of geotextile layers for each column	Confining pressure (kPa)
1	1	Sand50	Sand column material	----	50
	2*	Sand100			100
	3	Sand150			150
2	4	SB50	Surrounding loose soil bed	----	50
	5*	SB100			100
	6	SB150			150
3	7	OSC1	Surrounding soil reinforced by OSCs	A single column 0	100
	8*	OSC3		Three columns 0	
4	9*	HRSC1-2L	Surrounding soil reinforced by HRSCs	A single column – 2	100
	10	HRSC1-4L		4	
	11*	HRSC3-2L		Three columns – 2	
	12*	HRSC3-4L		4	
5	13*	VESC1	Surrounding soil reinforced by VESCs	A single column 0	100
	14	VESC3		Three columns 0	
6	15	SC-VE-2HL	Surrounding soil reinforced by a column with horizontal geotextile layers and vertical encasement simultaneously	2	100
	16	SC-VE-4HL		4	

*The tests which were performed two times to verify the repeatability of the test data

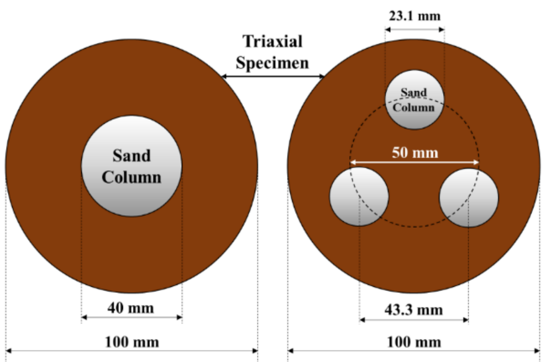

(a) Triaxial specimen with a single column and three columns

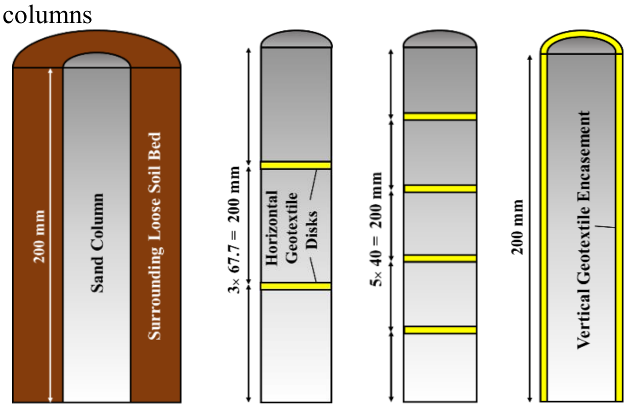

(b) a sample with a single OSC (c) HRSC (2 layers) (d) HRSC (4 layers) (e) VESC

Fig. 2 A typical test configuration for single and three columns

2.2 Testing program

The testing program consisted of sixteen independent consolidated undrained (CU) triaxial tests and was divided into six series of experiments (Table 3). In the first and the second series, the behavior of the Sand column material and the Surrounding soil bed under three different confining pressures (50, 100 and 150 kPa) were examined and their elastic modulus and shear strength parameters (Internal friction angle and cohesion) were determined. The third, 4th and 5th series was performed on composite specimens under confining pressure of 100 kPa and consisted of loose soil bed with single and three OSCs, HRSCs and VESCs, respectively. Finally, in the 6th series, a single column was reinforced with horizontal geotextile layers and vertical encasement simultaneously. Seven of the tests were repeated twice to examine the accuracy of the measurements, the performance of the apparatus and the repeatability of the system. The diameter of sand columns in specimens with single and three columns was assumed 40 and 23.1 mm, respectively, with an area replacement ratio of 16%. In practice, stone columns with a length-to-diameter ratio of between 4 and 20 are installed (FHWA 1983, Vetri selvan and Raj 2006, Aslani *et al.* 2018). This ratio for samples with one and three sand columns is 5 and 8.66, respectively.

In a field, stone columns are installed at a typical diameter range 0.5 to 1 m, with a typical particle size range 25 to 50 mm, so that the ratio of column diameter to particle size typically lies between 10 to 40 (Muir Wood *et al.* 2000). Also, Studies by Fox (2011) and Stoeber (2012) show that the minimum diameter of the column should be ten times the particle size. In the current study, this ratio (column diameter/ mean particle size) for specimens with single and three columns is 20 and 11.5, respectively, which the ratio is within this range (10-40) and conforms to these values in practice. It should be noted that the triaxial specimen is assumed as a unit cell only in the samples with a single column, while in the specimens with three columns, the diameter of the unit cell (D_e) can be calculated from Eq. (1).

$$D_e = 1.05S \qquad (1)$$

2.3 Preparation of specimens with single and three columns

Triaxial tests were performed on specimens with 100 mm diameter and 200 mm height. For preparing specimens, in all the tests the surrounding soil and sand column material were prepared at a water content of 10% and 4%, respectively. Also, the surrounding soil and sand column material were prepared at relative compaction of 78% (37% relative density) and 96% (77% relative density), respectively. According to Budhu's classification (Budhu, 2015), these two soils are respectively loose and dense soils. The sand column material has an adequate relative compaction and the surrounding soil has poor mechanical properties. Therefore the sand column can improve the bearing capacity of the loose specimen. Both soils were mixed well with water according to specific unit weight to

(a) Stage of sand columns construction in the triaxial mold

(b) Plastic tamper for the specimens with three sand columns

Fig. 3 Preparation of triaxial specimen and loading step

create homogenous materials. In the specimen with a single VESC (test VESC1), geotextile with a height of 200 mm was twisted away a Poly Vinyl Chloride (PVC) pipe (diameter of 40 mm) and the overlapping seam was stuck with glue, pipe was placed at the center of the mold (with inner diameter of 100 mm), and then surrounding soil was formed in three layers around the encased pipe. Each layer of the soil was determined by weight to achieve 78% relative compaction and compacted by the plastic tamper. Then pipe (without geotextile) was pulled out carefully and surrounding soil bed due to a little cohesion did not collapse. The smooth outer surface of the PVC pipe was lubricated with silicone grease to enable the free movement and reduce the friction and minimize the disturbance of surrounding soil during pull-out of pipe vertically from the specimen (Selvakumar and Soundara 2019). Similar to Deb *et al.* 2011, in this step the unit weight of sand column material was determined at 77% relative density and using the known volume of the hole, the total weight of sand required to fill up the hole was determined. The sand was smoothly charged into the hole in three equal batches and compacted using 15 mm diameter rod. The finished height of each batch was measured by a ruler and the weight of each batch was constant, hence compaction of the silica sand was controlled. The light compaction was adopted for silica sand to ensure that there was no significant lateral bulging of the column which created disturbance to the surrounding loose soil. In the test HRSC1-4L, the first batch was poured in the hole and compacted, a geotextile layer with 40 mm diameter was inserted, and each batch of sand similarly was compacted in such a manner that the finished height of each layer of the sand column was 40 mm. In the specimens reinforced by three columns, the overall steps of preparation were similar to a single column at the same area replacement ratio, and the exceptions were the PVC pipe diameter and plastic tamper shape. The view of the installation of three columns and plastic tamer is presented in Fig. 3. The method of column installation was selected in order to ensure the production of reasonably uniform columns. This method (compaction of sand into a pre-bored hole without drilling) was used by many researchers (Malarvizhi and Ilamparuthi 2007, Frikha *et al.* 2014 and Frikha *et al.* 2015).

After preparing samples and Test setup, Shear loading was applied at a deformation rate of 1mm/min under constant confining pressure.

3. Numerical simulation

To perform the analysis, three–dimensional finite element models of the laboratory tests (samples without and with one and three OSCs, HRSC and VESC) were simulated (Fig. 4) using a commercial package ABAQUS 6.14-2. For this propose, cylinders with 100 mm diameter and 200 mm height were modeled using a finite element method (FEM). Sensitivity analysis was conducted using different element sizes before adopting mesh discretization for various group configurations. Based on this study, element approximate size for surrounding soil and column were selected 10 mm and 6 mm, respectively. Components of the composite specimens were simulated by using C3D20R (20-node quadratic brick, reduced integration elements). Table 4 shows the properties of various materials used for numerical simulation. Mohr-Coulomb's elasto-plastic failure criterion with non-associated flow rule was adopted for surrounding loose soil bed and sand column materials. Young's modulus and shear strength parameters are obtained from the triaxial tests. Poisson's ratio of loose sands ranges from 0.15 to 0.35 m (Das 2008) and the average value was applied for soil bed, while for sand column material, Poisson's ratio was estimated adopting the Eq. (2) proposed by Trautmann and Kulhawy (1987). In this equation, φ_{sc} is the friction angle of the sand column material in the triaxial test.

$$\nu = 0.1 + 0.3\left(\frac{\phi_{sc} - 25^{\circ}}{45^{\circ} - 25^{0}}\right) \tag{2}$$

The linear elastic material was used for geotextile and yielding of the reinforcements was not considered, as none was observed in the model tests (Demir *et al.* 2014). Poisson's ratio for the geotextile was obtained from the literature as 0.3 (Keykhosropur and Imam 2012, Debnath and Dey 2017) and the elastic modulus (E_g) was calculated using Eq. (3) and Table 2.

$$J = E_g t \tag{3}$$

where J and t are the stiffness and the thickness of the geotextile, respectively. It should be noted that Young's modulus of surrounding loose soil in confining pressures of 50 and 150 kPa is 0.6 and 1.5 MPa, respectively, and for sand column materials these values are 8 and 20 MPa, respectively. The values of Young's modulus for the surrounding soil and the sand column materials (and especially their ratio) are in good agreement with the values presented by other researchers (Hassen *et al.* 2010, Han *et al.* 2007, Guetif *et al.* 2007). This comparison demonstrates the positive effect of the sand column as a soil improvement technique for the loose soil.

Based on similarity analysis rules and the scale effect concept, the value of the non-dimensional parameters for small scale model tests and large scale granular columns must be the same. One of the non-dimensional parameters is defined as Eq. (4).

$$SF = \frac{E_{sc} D}{J} \tag{4}$$

where SF is the scale factor, and E_{sc} is the sand/stone Young's modulus. The value of SF for this study and previous researches is summarized in Table 5.

Table 4 Material properties used in numerical models

	Loose soil bed	Sand column material	Geotextile
Unit weight (kN/m^3)	15.1	17.5	1.8
Young's modulus (MPa)	1*	15*	130
Poisson's Ratio (ν)	0.25	0.27	0.3
Internal friction angle (φ)	21°	36°	----
Dilation angle (ψ)	0	6°	----
Cohesion (kPa)	2	0	----

*Young's modulus of soils under confining pressure of 100 kPa

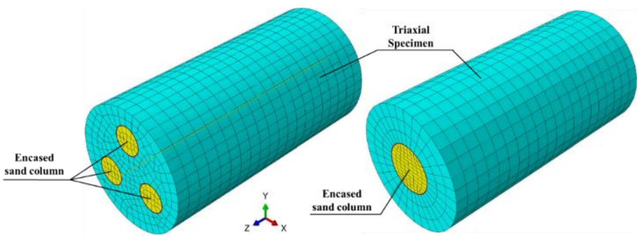

Fig. 4 Complete 3D mesh geometry of the finite element model

Table 5 the scale factor in other researches

Study		D (m)	E_{sc} (MPa)	J (MN/m)	SF
Ghazavi and Nazariafshar (2013)		0.6	40	5	4.8
Zhang and Zhao (2014)		0.8	45	2.5	14.4
Debnath and Dey (2017)		0.05	44	0.21	10.47
Kadhim *et al.* (2018)		0.15	25	0.4	9.37
This study	a Single column	0.04	15	0.052	11.53
	Three columns	0.023	15	0.052	6.63

The scale factor presented in this study is within a range of field values or small-scale model tests values presented by other researchers. Hence, the stiffness and properties of all materials were scaled down. It may be difficult to use a single scale factor to extrapolate the results. Nevertheless, a relation between different model dimensions and the prototype dimensions can be established, where the scale factor would be different. These respective scale factors may be applied to scale up the model test results (Mazumder *et al.* 2018, Alkhorshid *et al.* 2019). The interface between the soils and the vertical geotextile encasement were assumed to be full contact because they are tightly interlocked (Debnath and Dey 2017, Castro 2017, Tang *et al.* 2015, Lo *et al.* 2010). Also, considering a tight interlocking of the sand columns with the surrounding soil (mixed zone), this interaction was assumed perfect (tie constraints) and at the interfaces, no separation or slip was allowed (Ambily and Gandhi 2007, Shahu and Reddy 2011, Castro 2017). At the soils-vertical encasement interfaces deformation of the column is mainly by radial bulging and no significant shear is possible (Ambily and Gandhi 2007). On the other hand, horizontal geotextile reinforcement disks provide the lateral confinement to the columns against bulging by friction mobilization and slip can occur at the sand-disks interfaces. Therefore, a penalty friction formulation, based on Coulomb's friction law, was used as the contact property, indicating the frictional behavior between sand column material and horizontal disks. The contact interface is characterized by the friction coefficient (μ). In the numerical model, the coefficient of friction was assumed to be 0.49, and the value corresponds to the empirical relation (Eq. (5)). This parameter is calculated for each soil separately and is assigned at the soils-geotextile interfaces. It should be noted that in this numerical analysis, the geotextiles were simulated using solid elements (Debnath and Dey 2017).

$$\mu = 2/3 \tan(\phi) \tag{5}$$

This estimation is adopted in the routine design of geosynthetic-reinforced soil structure when laboratory data is lacking (Lee *et al.* 2010). For the boundary conditions and loading step, first confining pressure was applied to the top of the specimen and its Sides surface, and then in the shear step, the top surface of the sample is finally compressed 3 cm (the axial strain of 15%). The bottom surface of the specimen is fixed at all stages of loading.

4. Results and discussion

4.1 Repeatability of the test results

Repeatability of the test results in experimental studies is an important problem in order to attain trustful data. Fig. 5 presents some of the duplicate tests and depicted a close match between results of the two trial tests with maximum differences of around 9.2% (this difference was considered to be small and is subsequently neglected). This process shows that the procedure adopted can produce repeatable tests within the bounds that expected from testing apparatuses.

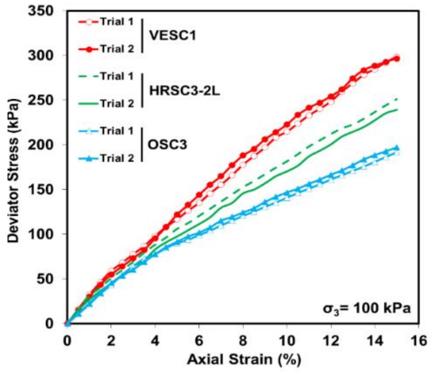

Fig. 5 Repeated tests to examine the accuracy of the measurements under confining pressure of 100 kPa

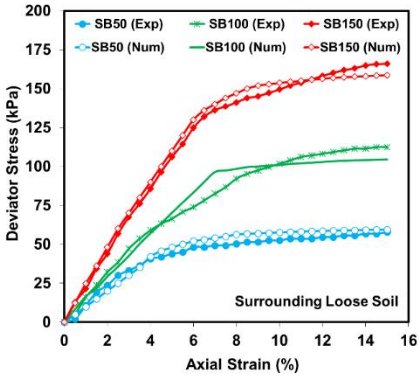

(a) Surrounding loose soil behavior

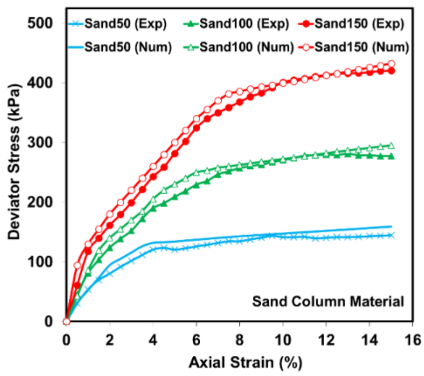

(b) Sand column material behavior

Fig. 6 Comparison between numerical analysis and experimental stress–axial strain curves in confining pressures of 50, 100, and 150 kPa

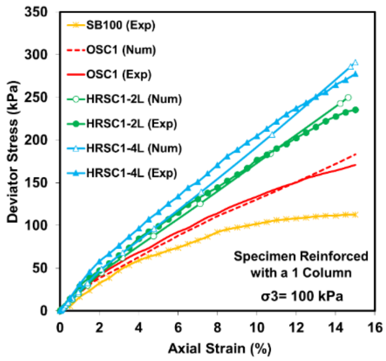

(a) Single column behavior

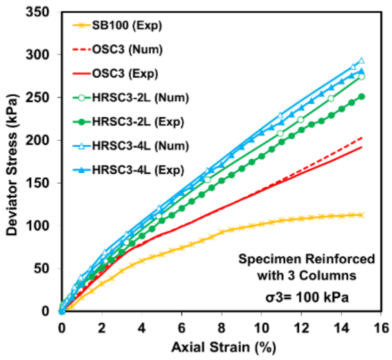

(b) Three columns behavior

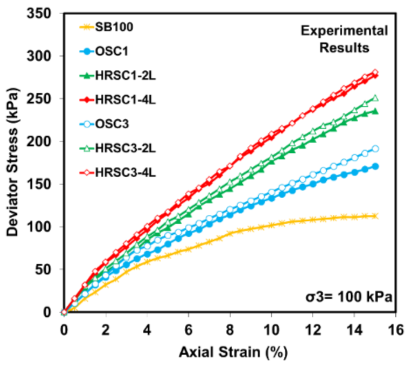

(c) Comparison between single and three columns behavior

Fig. 7 Stress–axial strain curves derived from the numerical analysis and experimental tests on specimens reinforced by columns with two and four layers of geotextile in confining pressures of 100 kPa

4.2 Surrounding soil and sand column material behavior

Many authors reported spread loading conditions (embankments) in their triaxial tests with confining pressures of 50 to 200 kPa (Najjar *et al.* 2010, Nguyen *et al.* 2013, Xue *et al.* 2019). Fig. 6 shows the deviator stress-axial strain curves of the surrounding loose soil and sand column material specimens resulting from the experimental and numerical analysis under three different confining pressures. Since no maximum deviator stresses were reached during the triaxial tests, failure was defined at an axial strain of 15%. Fig. 6 reveals that the results of the numerical analysis are in good agreement with experimental data so that at most strain levels, there is a difference of less than 20% between experimental and numerical results.

4.3 Effect of laminated geotextile reinforcement

Fig. 7 shows deviator stress-strain variations of samples containing one and three HRSCs resulting from numerical and experimental analysis at a confining pressure of 100 kPa. Fig. 7 indicates that the single OSC improved the strength of the loose soil specimen about 52% and increased the flexibility and load-bearing of the samples, especially in higher strain level (5% to 15%). Also, as shown in Figs 7(a)-7(b) the experimental test results match well with the numerically predicted responses. Changing the number of horizontal layers from 2 to 4 resulted in the ultimate bearing capacity of the specimen to increase by 17 and 12 percent for specimens with one and three columns, respectively. Hence, the efficiency of horizontal geotextile layers on bearing capacity improvement enhances with increasing the number of horizontal layers and they are placed at shorter intervals.

4.4 Effect of geotextile encased column

Deviator stress-strain curves for the specimen with single and three VESCs and HRSCs (4 layers) under 100 kPa confining pressure have been shown in Fig. 8. In the single VESC due to the additional confinement produced by the geotextile, the bearing capacity was improved compared with a single OSC, so that experimental results showed that for the 2.5%, 5%, 7.5%, 10%, 12.5% and 15% strain level, increase in the bearing capacity of the sample was about 38%, 45%, 51%, 60%, 67% and 74%, respectively. Therefore the beneficial effect of vertical encasements to enhance the shear stress of specimens appear clearly in higher strain level. It can be seen in Fig. 8(a) that four Horizontal reinforcing layers achieved a similar performance to a vertical encasement geotextile, in terms of strength improvement. The ratio of ultimate strength (in the 15% strain level) of specimens with VESCs to the ultimate strength of specimens with HRSCs (4 layers) for samples with single and three columns were 7% and 12%, respectively. Indeed, using a geotextile as vertical encasement provides no significant increase in specimen's strength against four horizontal layers. On the other hand, the geotextile needed for encasing the single and three columns are around 5 and 6.8 times of the geotextile required for four layers, respectively. Therefore, the vertical

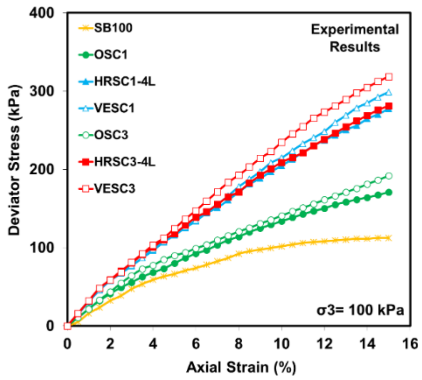

(a) Comparison between four laminated disks and geotextile encasement

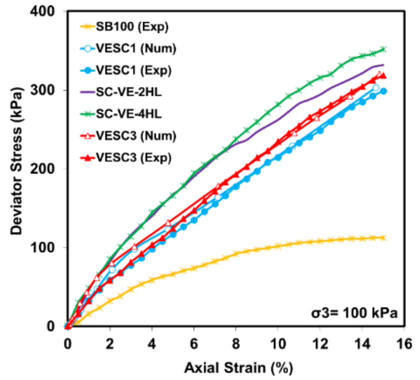

(b) Use of geotextile layers and encasement simultaneously

Fig. 8 Stress–axial strain curves for specimens reinforced by single and three columns under confining pressure of 100 kPa

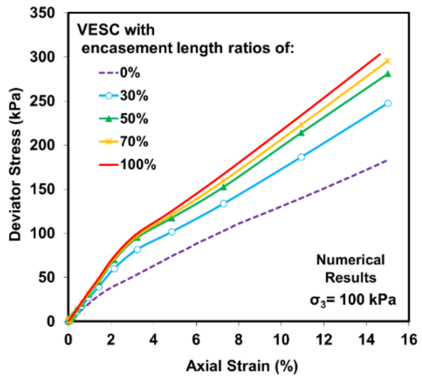

Fig. 9 Stress-axial strain curves derived from numerical analysis on specimens reinforced by an encased single column in different geotextile encasement lengths under 100 kPa confining pressure

Table 6 Strength Improvement Factor (IF_S) in confining pressure of 100 kPa from FEM

	Number of layers in a HRSC			ELR in a VESC			
	0	2	4	30%	50%	70%	100%
IF_S	1	1.36	1.59	1.37	1.55	1.63	1.68
A_g (cm^2)	0	25.13	50.26	62.83	125.66	188.50	251.33

geotextile encasement (at 100% of column's length)

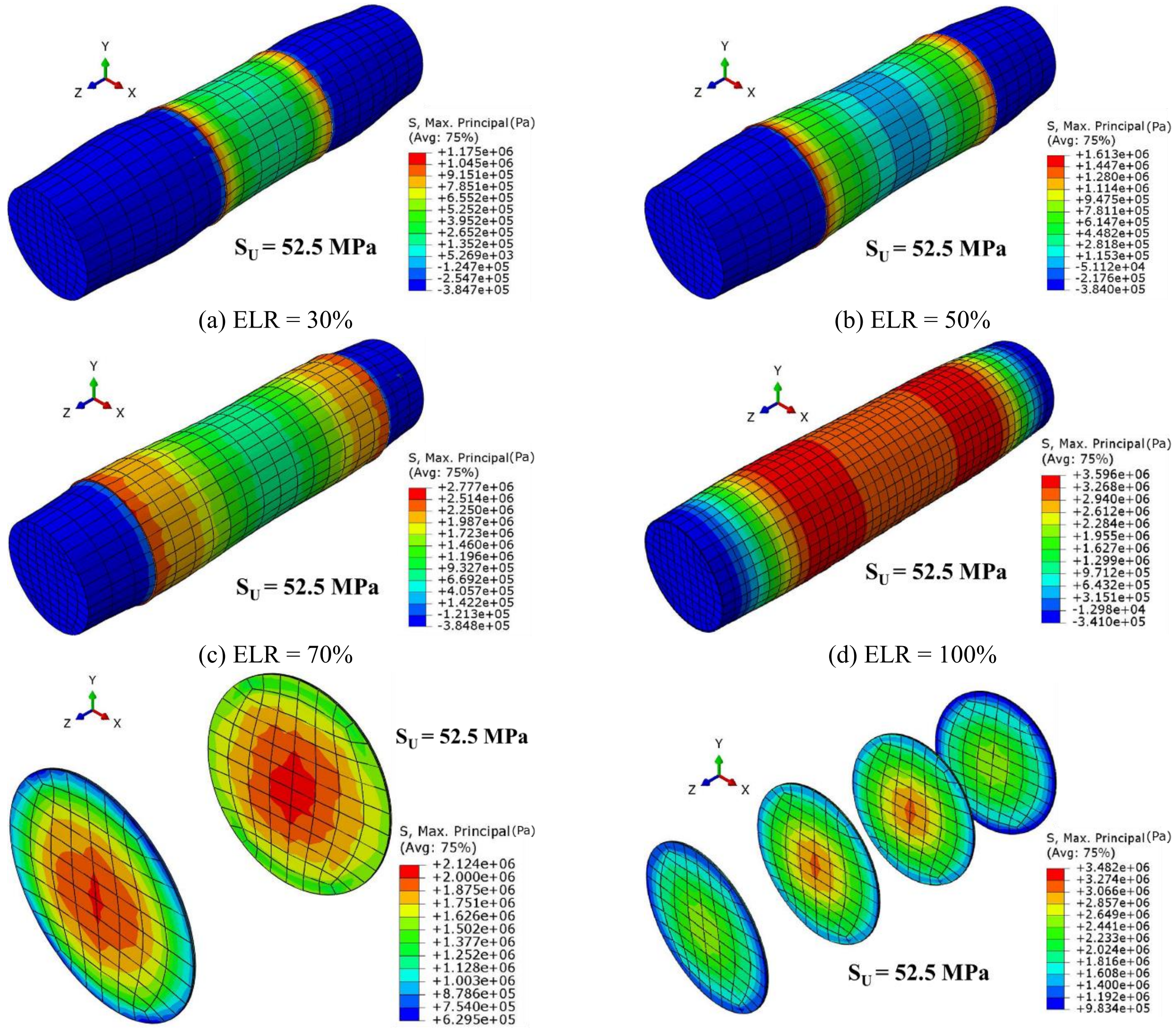

(a) ELR = 30% (b) ELR = 50%

(c) ELR = 70% (d) ELR = 100%

(e) 2 Horizontal reinforcing layers (f) 4 Horizontal reinforcing layers

Fig. 10 Maximum principal stress of the single column in triaxial composite samples

compared with the four horizontal layers does not seem to be economical. Fig. 8(b) illustrates a good agreement between the results of the experiment and the numerical analysis, regardless of the number of sand columns. The ultimate bearing capacity of specimens with a single VESC (test VSCE1), a HRSC with 4 layers (test HRSC1-4L) and the specimen reinforced by a column with 4 horizontal layers and vertical encasement simultaneously (test SC-VE-4HL) were 299kPa, 281kPa and 352 kPa, respectively.

Hence, the use of horizontal geotextile layers and vertical encasement simultaneously increases the strength of samples compared to other reinforced states (only geotextile layers or only encasement), but this increase in load-bearing capacity is much less than the total summation of the bearing capacity of each of these states alone.

In order to investigate the effect of vertical encasement in different lengths (located in the middle of the column where maximum bulging occurred) numerical simulations were conducted. The ratio of the length of vertical encasement to column length is defined as the encased length ratio (ELR).

Fig. 9 illustrates the deviator stresses-axial strain variations for specimens with a single VESC in different encased length ratios. It can be seen in this figure that the strength of samples increases with increases in ELR. However, reinforcement over 50% of the column length, especially for strain levels less than 5% (design strain levels), has no significant effect on the load bearing capacity improvement of the specimen. The maximum principal stress contours for the deformed VESC in the composite samples with different ELR and horizontal geotextile layers (2 and 4 disks) at 15% strain under 100 kPa confining pressure are shown in Figs. 10(a)-(d) and Figs. 10(e)-(f), respectively. As expected, with the increase in ELR, the concentration of tensile stress (with a positive sign) in geotextiles increases. Also, with the increase in ELR from 0% to 100% the maximum column bulging is controlled and its location occurrence is transmitted from 2.5D to about 1.2D.

In a real project, it can be used partially VESCs in loose layered soil and transmit the local lateral bulging to dense soil layers. When horizontal geotextile layers are

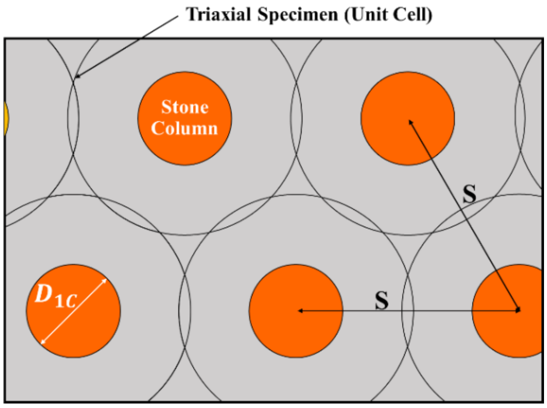

(a) Specimen reinforced by a single column with complete equilateral triangular arrangement

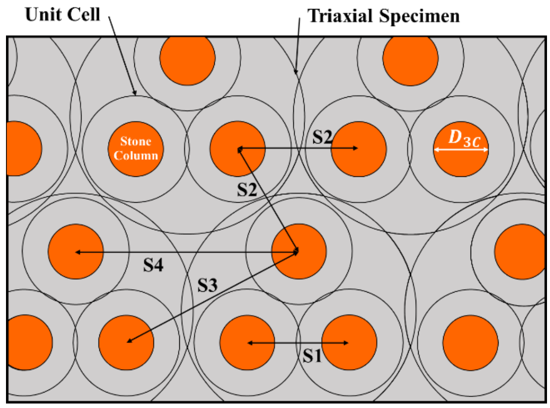

(b) Specimen reinforced by three columns with incomplete triangular arrangement

Fig. 11 The pattern of granular columns in the widespread field based on unit cell concept

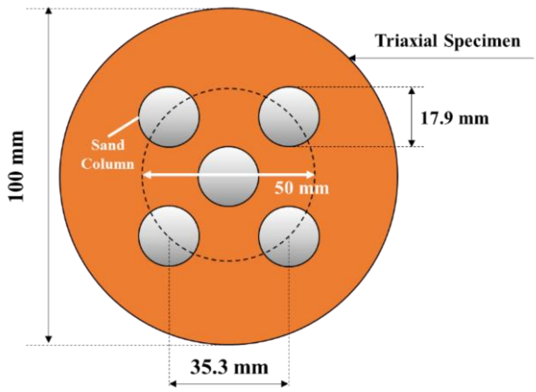

(a) Arrangement of five columns in the triaxial specimen

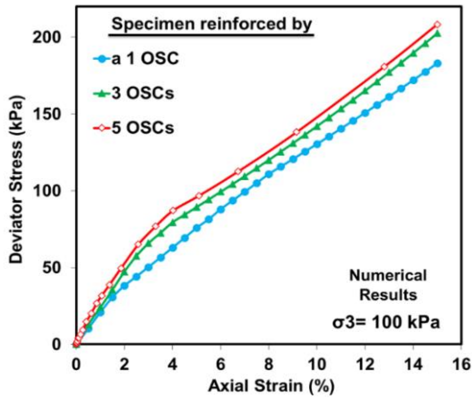

(b) Deviator stress–axial strain curves for specimens with 1, 3 and 5 unreinforced columns

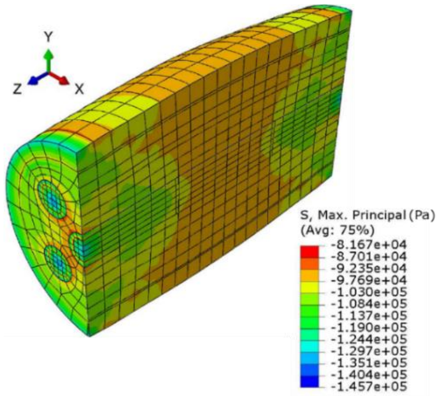

(c) Maximum principal stress at 15% strain level

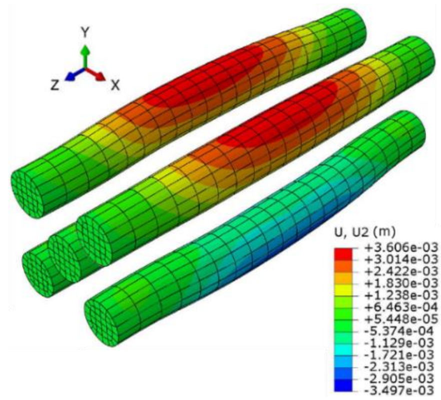

(d) Displacement of the 5 columns in the y–direction

Fig. 12 specimen with five columns under 100 kPa confining pressure

used, column bulging is locally restricted by friction mobilization on the geotextile surface. The stresses in the geotextiles at the end of the analysis are always much lower than the geotextile's ultimate stress (S_U). This implies the primarily elastic behavior of the geotextiles during the triaxial loading. With comparing the tensile stress of horizontal layers and vertical encasement, it can be concluded that the stress distribution in the horizontal disks is more appropriate than the vertical encasement, so that the maximum tensile stress mobilized in four geotextile layers is about 2.1 times the maximum tensile stress mobilized in the geotextile with ELR = 50%. In other words, the horizontal layers use more their tensile strength than the vertical encasement. Table 6 presents the performance of reinforced samples with a HRSC (in a different number of layers) and a VESC (in different encasement length ratios) with the amount of geotextile consumed (A_g). In this table, IF_S is defined as the ratio of the ultimate strength (in the 15% strain) of the specimens with a single reinforced sand column to the ultimate strength of the sample with a single OSC derived from the numerical analysis. As seen, the sample containing a HRSC with four geotextile layers

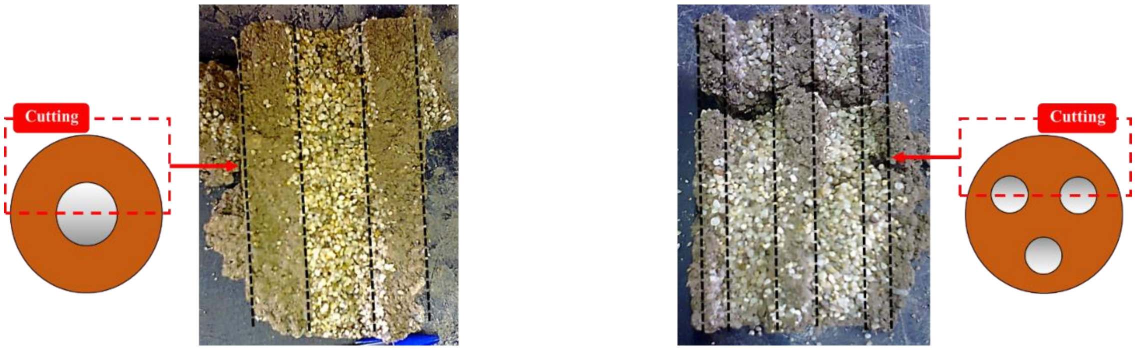

(a) A single column failure (b) Three columns failure

Fig. 13 Observed failure of the unreinforced sand columns subjected to the triaxial test

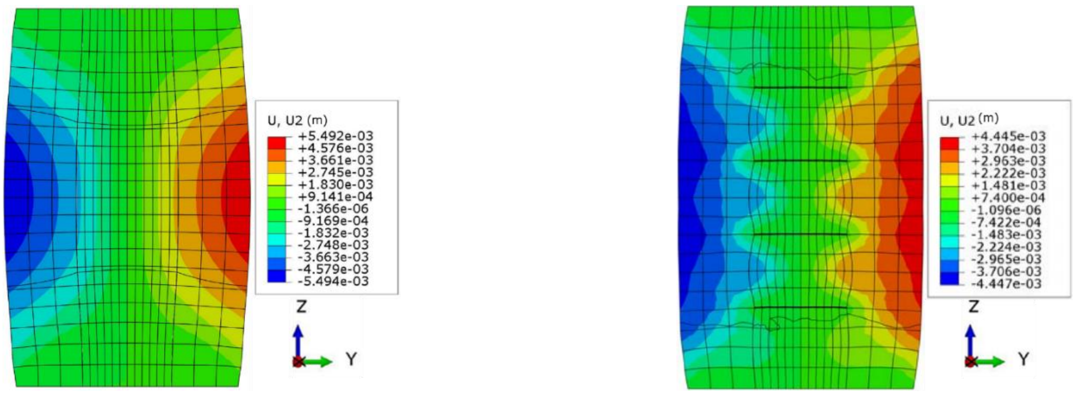

(a) The specimen with an OSC (b) The specimen with a HRSC with 4 disks

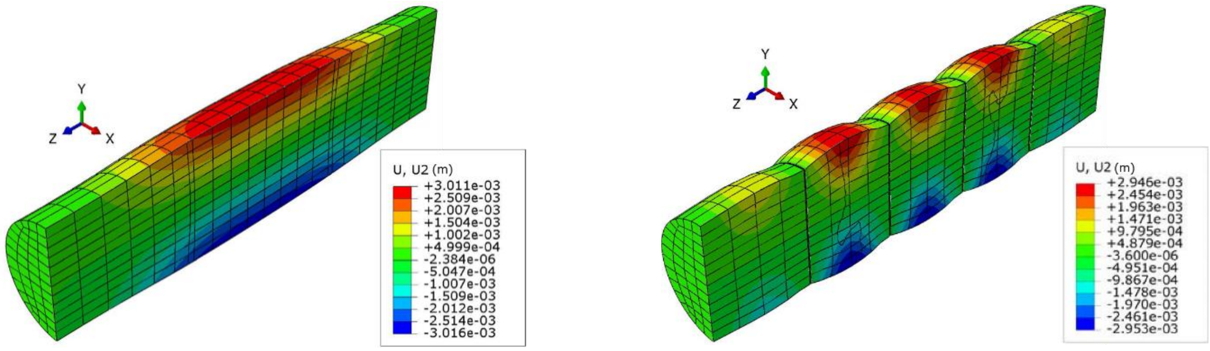

(c) A single OSC (d) A HRSC with 4 disks

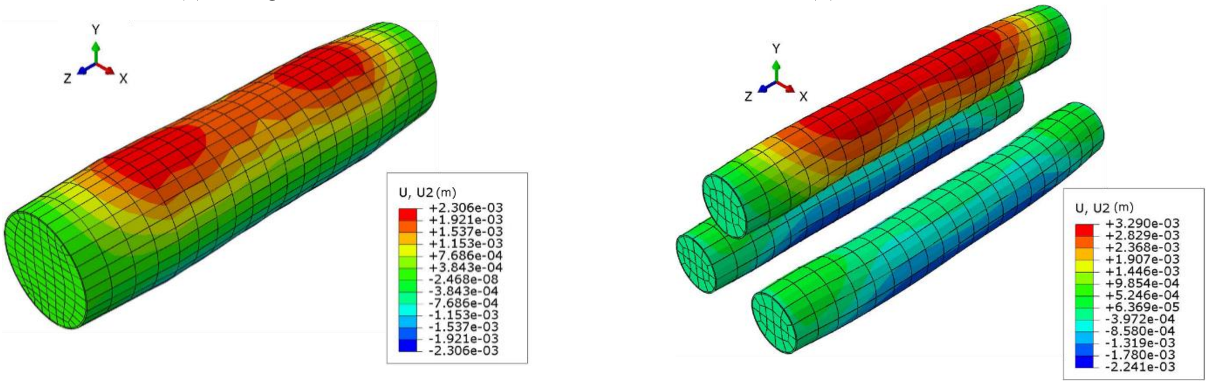

(e) A single VESC (f) Three VESCs

Fig. 14 Displacements of the specimen/columns in the y-direction

achieved similar performance to the specimen containing a VESC with ELR = 50%, while, in this case the geotextile area required for vertical encasement is 2.5 times that of horizontal disks. Therefore, it can be said that, with regard to economic considerations, the use of horizontal disks as a vertical encasement is a priority.

Table 7 Bulging Improvement Factor (IFB) in confining pressure of 100 kPa from numerical analysis

Sample with:	a single column							3 columns				5 columns
	Number of disks			ELR				Number of disks			ELR	ELR
	0	2	4	30%	50%	70%	100%	0	2	4	100%	0%
IF_B	1.11	1.28	1.37	1.31	1.40	1.44	1.46	1.14	1.30	1.40	1.48	1.16

4.5 Effect of the number of sand columns with the same area replacement ratio

As shown in Figs. 7(c) and 8(a), Comparison between two different types of reinforced specimens (a single column and three columns with the same area replacement ratio) reveals that with increasing the number of columns the increase in deviator stress is insignificant. For example, at the strain level of 5%, the shear stress of specimens with single and three unreinforced columns are, respectively, 1.21 times and 1.35 times of surrounding loose soil specimen. This result also is observed qualitatively in Frikha *et al.* (2015) study. Based on unit cell approach, the specimens with single and three columns can arrange in an actual widespread field similar to Fig. 11(a) and Fig. 11(b), respectively. For example, in a real project assuming the group of granular columns with diameters of 1 m and complete equilateral triangular pattern (D_{1C} = 1 m in Fig. 11(a)), the diameter of the small columns for incomplete triangular pattern is calculated 0.58 m (D_{3C} = 0.58 m in Fig. 11(b) due to the fixed area replacement ratio). In this case, amounts of S1, S2, S3, and S4=S will be 1.07, 1.27, 2.07 and 2.38 m respectively. Previous studies (Hughes and Withers 1974, Gniel and Bouazza 2009, Dash and Bora 2013) show that for the group performance of stone columns, the spacing of the columns should be shorter than 2.5 times of column diameter (i.e., 2.5 m for the complete equilateral triangular pattern and 1.45 m for incomplete triangular pattern). Thus in Fig. 11(b) the columns with a spacing larger than 1.45 m (S3 and S4), the group performance does not matter and the soil mass beyond this distance is not influenced by the loading on the columns. Although the columns in the specimen with three columns have a suitable arrangement, due to the large spacing between the columns in the widespread field (S3 and S4) the strength of this specimen is close to the specimen with a single column, regardless of the form of the reinforcements (horizontal geotextile layers or vertical encasement). In a real project, the cost of penetration for three columns (a representative of the sample with three columns) is at least 2-3 times the cost of a single penetration (representative of the sample with a single column) with the same area replacement ratio, and in terms of strength, there is no significant difference between the two patterns (Figs. 11(a)-(b)). Therefore, in a widespread field with loose soil bed, if the granular column materials are constant, it is better to group of columns in a complete equilateral triangular arrangement is used, instead of using a group of columns with an incomplete triangular pattern and a smaller diameter. In order to investigate the non-economic accuracy of multi-column samples with incomplete triangular pattern compared to the samples with a complete triangular arrangement, the sample containing five sand columns is simulated. Fig. 12 shows the deviator stress-axial strain curves of samples containing one, three, and five OSCs under 100 kPa confining pressure and maximum principal stress and displacement (in y-direction) contours of the specimen with five OSCs resulting from the numerical analysis.

In Fig. 12(c), the stress concentration in the sand column is observed due to the difference in the elasticity modulus of the soils (sand column and surrounding soil). Also, according to Fig. 12(b), there is no significant difference between the strength of the multi-column specimens and specimen with a single OSC (maximum percentage difference is 14%). specimens with three and five columns (the incomplete pattern in the widespread field) are not cost-effective, especially when using VESCs. Value of geotextile used for three and five VESCs is 73% and 123% higher than a single VESC.

4.6 Effect of the reinforcements on column bulging

The failure mechanisms of the end bearing columns can occur in three different ways: shear failure, bulging failure, and lateral spreading. An end bearing stone column less than about 2 to 3 diameters in length may fail in shear mode before a bulging failure can develop (FHWA 1983). Therefore there is no possibility of shear failure. Fig. 13 shows a cross-section of a surrounding loose soil specimen reinforced by a single OSC and three OSCs in the post-failure phase. This figure demonstrates that with the increase in deviator stress the surrounding loose soil specimens failed due to the bulging and lateral spreading of the sand columns.

The deformed shapes of the samples/columns at 15% strain under confining pressure of 100 kPa are shown in Fig. 14. Although the bulging of the HRSC is close to the OSC (Figs. 14(c)-(d)), the lateral deformation of the sample contains a HRSC is much less than a sample with an OSC (Figs. 14(a)-(b)). The reason for this is the occurrence of local bulging at intervals between disks (short length = 5 cm) for HRSC and the occurrence of general bulging along the entire length of the column (20 cm) for OSC due to the lack of adequate confinement. As observed in Figs. 14(e)-(f) the lateral bulging of three thin VESCs is 42% more than a single thick OSC in the triaxial samples. In the VESC with ELR = 100% there is higher resistance against bulging resulting from the hoop stresses in the geotextile. In order to evaluate the effect of the reinforcements on samples bulging the ratio of maximum lateral deformation of the surrounding loose soil specimen to maximum lateral deformation of reinforced specimens at 15% strain level under 100 kPa confining pressure is defined as the Bulging Improvement Factor (IF_B). The amounts of IF_B for all specimens from the numerical analysis presented in Table 7.

As seen in this table, the full vertical encasement (ELR = 100%) compared to the four horizontal disks is only about 7% less effective in reducing the bulging of the sample. Also, the bulging of the sample with a single column is almost 3% higher than the sample with three columns. Therefore, the number of reinforcing columns with the constant volume of the sand column materials has no significant effect on the bulging and bearing capacity of the loose soil triaxial specimens.

5. Limitations

There are several limitations in this paper, as described in the following:

• Although the use of stone columns has different applications such as drainage and increase the rate of consolidation in the soft bed, current research works mainly emphasize the load-bearing capacity of the granular columns. Therefore, triaxial tests were performed on the specimens in the low moisture content (4% and 10% for the sand column and surrounding soil, respectively) and without measuring the excess pore-water pressure.

• In spite of many studies on the behavior of the granular column under triaxial tests (these studies were presented in the Introduction section), as the triaxial samples are too small to represent the widespread field, hence the results obtained from this paper may not be representative of in situ performance and were used in the context of the comparative study.

• The results of this research are obtained for only one type of geotextile and soils with specific mechanical properties. Therefore, if the properties of each of the materials (geotextile, stone column materials and surrounding soil) were changed, although it can be expected that the results have the same general trend, additional experiments should be performed.

6. Conclusions

This paper reported the experimental study and the numerical analysis of specimens containing loose soil with a single column and three columns in 16% area replacement ratio. Sand columns reinforced by vertical geotextile encasement and horizontal layers increased the bearing capacity of the composite specimen. The following conclusions were obtained from the experimental and numerical study:

1. The results indicated that for a given value of area replacement ratio, the number of columns has little effect on the shear strength of the specimen with reinforced or unreinforced columns in each strain level. The ultimate bearing capacity of the sample with five OSCs is eventually about 14% more than samples with a single OSC.

2. Based on unit cell approach in the loose widespread field with the assumption that the volume of the stone column materials is constant, using a group of granular columns with the complete equilateral triangular arrangement can give better performance (from the viewpoint of the bearing capacity improvement) than a group of granular columns with the incomplete triangular pattern. The cost of penetrating by vibrator for three columns is at least 2-3 times the cost of a single column. Also, the value of geotextile used for three VESCs is 73% higher than a single VESC.

3. Reinforcing the sand columns by either horizontal layers or vertical encasement increases the flexibility and load-bearing of the samples compared to the OSCs. Comparison between two reinforcement modes (VESCs and HRSCs) exhibit that at various strain levels the shear stress of the specimen reinforced by HRSC with four geotextile layers with a shear stress of the specimen containing a VESC with ERL = 50% encasement is approximately equal. The geotextile area required for a VESC is 2.5 times that of a HRSC. It should be noted that given the low stress level in the geotextiles, it can be concluded that the geotextiles remain elastic during the triaxial loading, regardless of reinforcement mode.

4. With the increase in ELR from 0% to 100% the maximum column bulging is controlled and its location occurrence is transmitted from 2.5D to about 1.2D. In a real project, it can be used partially VESCs in loose layered soil and transmitted the local lateral bulging to dense soil layers.

5. The bearing capacity the single VESC was improved compared with a single OSC, so that experimental results showed that for the 5%, 10% and 15% strain level, increase in the bearing capacity of the sample was about 45%, 60% and 74%, respectively. Hence, increasing the strain level, the benefit of encasement increases and the high strain levels should be imposed to clearly appear the effect of vertical geotextile encasement.

The combined use of two types of geotextiles (horizontal geotextile layers and vertical encasement simultaneously) increases the bearing capacity of samples compared to other reinforced states (only horizontal layers or only vertical encasement), but this improvement in strength is much lower than the total summation of the strength of each of these states alone.

References

Ali, K., Shahu, J.T. and Sharma, K.G. (2012), "Model tests on geosynthetic-reinforced stone columns: a comparative study", *Geosynth*. *Int*., **19**(4), 292-305. http://dx.doi.org/10.1680/gein.12.00016.

Ali, K., Shahu, J.T., Sharma, K.G. (2014), "Model tests on single and groups of stone columns with different geosynthetic reinforcement arrangement", *Geosynth*. *Int*., **21**(2), 103-118. http://dx.doi.org/10.1680/gein.14.00002.

Alkhorshid, N.R., Araujo, G.L., Palmeira, E.M. and Zornberg, J.G. (2019), "Large-scale load capacity tests on a geosynthetic encased column", *Geotext*. *Geomembr*., 103458. https://doi.org/10.1016/j.geotexmem.2019.103458.

Ambily, A.P. and Gandhi, S.R. (2007), "Behavior of stone columns based on experimental and FEM analysis", *J*. *Geotech*. *Geoenviron*. *Eng*., **133**(4), 405-415. https://doi.org/10.1061/(ASCE)1090-0241(2007)133:4(405).

Aslani, M., Nazariafshar, J. and Ganjian, N. (2019), "Experimental study on shear strength of cohesive soils reinforced with stone columns", *Geotech*. *Geol*. *Eng*., **37**(3), 2165-2188. https://doi.org/10.1007/s10706-018-0752-z.

Barksdale, R.D. and Bachus, R.C. (1983), "Design and

Construction of Stone Columns Volume I", Federal Highway Administration Report FHWA. RD-83/026; National Technical Information Service, Springfield, Virginia, U.S.A.

Black, J.A., Sivakumar, M.R., Madhav, M.R. and Hamiil, G.A. (2007a), "Reinforced stone columns in weak deposits: Laboratory model study", *J. Geotech. Geoenviron. Eng.*, **133**(9), 1154-1161. https://doi.org/10.1061/(ASCE)1090-0241(2007)133:9(1154).

Black, J.A., Sivakumar, V. and Bell, A. (2011), "The settlement performance of stone column foundations", *Géotechnique*, **61**(11), 909-922. https://doi.org/10.1680/geot.9.P.014.

Black, J.A., Sivakumar, V. and McKelvey, D. (2007b), "Performance of clay samples reinforced with vertical granular columns", *Can. Geotech. J.*, **44**(1), 89-95. https://doi.org/10.1139/t06-081.

Budhu, M. (2015), *Soil Mechanics Fundamentals*. John Wiley & Sons.

Castro, J. (2017), "Groups of encased stone columns: Influence of column length and arrangement", *Geotext. Geomembr.*, **45**(2), 68-80. https://doi.org/10.1016/j.geotexmem.2016.12.001.

Cengiz, C., Kilic, I.E. and Guler, E. (2019), "On the shear failure mode of granular column embedded unit cells subjected to static and cyclic shear loads", *Geotext. Geomembr.*, **47**(2), 193-202. https://doi.org/10.1016/j.geotexmem.2016.12.001.

Das, B.M. (2013), *Advanced Soil Mechanics*, CRC Press.

Dash, S.K. and Bora, M.C. (2013), "Influence of geosynthetic encasement on the performance of stone columns floating in soft clay", *Can. Geotech. J.*, **50**(7), 754-765. https://doi.org/10.1139/cgj-2012-0437.

Deb, K. and Majee, A. (2014), "Probability-based design charts for stone column-improved ground", *Geomech. Eng*, **7**(5), 539-552. http://dx.doi.org/10.12989/gae.2014.7.5.539.

Deb, K., Samadhiya, N.K. and Namdeo, J.B. (2011), "Laboratory model studies on unreinforced and geogrid-reinforced sand bed over stone column-improved soft clay", *Geotext. Geomembr.*, **29**(2), 190-196. https://doi.org/10.1016/j.geotexmem.2010.06.004.

Debnath, P. and Dey, A.K. (2017), "Bearing capacity of geogrid reinforced sand over encased stone columns in soft clay", *Geotext. Geomembr.*, **45**(6), 653-664. https://doi.org/10.1016/j.geotexmem.2017.08.006.

Demir, A. and Sarici, T. (2017), "Bearing capacity of footing supported by geogrid encased stone columns on soft soil", *Geomech. Eng.*, **12**(3), 417-439. https://doi.org/10.12989/gae.2017.12.3.417.

Demir, A., Yildiz, A., Laman, M. and Ornek, M. (2014), "Experimental and numerical analyses of circular footing on geogrid-reinforced granular fill underlain by soft clay", *Acta Geotechnica*, **9**(4), 711-723. https://doi.org/10.1007/s11440-013-0207-x.

Fattah, M.Y., Zabar, B.S. and Hassan, H.A. (2016), "Experimental analysis of embankment on ordinary and encased stone columns", *Int. J. Geomech.*, **16**(4), 04015102. https://doi.org/10.1061/(ASCE)GM.1943-5622.0000579.

Fox, Z.P. (2011), "Critical state, dilatancy and particle breakage of mine waste rock", Ph.D. Dissertation, Colorado State University, Fort Collins, Colorado, U.S.A.

Frikha, W., Bouassida, M. and Canou, J. (2014), "Parametric study of a clayey specimen reinforced by a granular column", *Int. J. Geomech.*, **15**(5), 04014078. https://doi.org/10.1061/(ASCE)GM.1943-5622.0000419.

Frikha, W., Tounekti, F., Kaffel, W. and Bouassida, M. (2015), "Experimental study for the mechanical characterization of Tunis soft soil reinforced by a group of sand columns", *Soils Found.*, **55**(1), 181-191. https://doi.org/10.1016/j.sandf.2014.12.014.

Ghazavi, M. and Afshar, J.N. (2013), "Bearing capacity of geosynthetic encased stone columns", *Geotext. Geomembr.*, **38**, 26-36. https://doi.org/10.1016/j.geotexmem.2013.04.003.

Ghazavi, M., Yamchi, A.E. and Afshar, J.N. (2018) "Bearing capacity of horizontally layered geosynthetic reinforced stone columns", *Geotext. Geomembr.*, **46**(3), 312-318. https://doi.org/10.1016/j.geotexmem.2018.01.002.

Gniel, J. and Bouazza, A. (2009), "Improvement of soft soils using geogrid encased stone columns", *Geotext. Geomembr.*, **27**(3), 167-175. https://doi.org/10.1016/j.geotexmem.2008.11.001.

Gu, M., Han, J. and Zhao, M. (2017), "Three-dimensional discrete-element method analysis of stresses and deformations of a single geogrid-encased stone column", *Int. J. Geomech.*, **17**(9), 04017070. https://doi.org/10.1061/(ASCE)GM.1943-5622.0000952.

Guetif, Z, Bouassida, M. and Debats, J.M. (2007), "Improved soft clay characteristics due to stone column installation", *Comput. Geotech.*, **34**(2), 104-111. https://doi.org/10.1016/j.compgeo.2006.09.008.

Han, J., Oztoprak, S., Parsons, R.L. and Huang, J. (2007), "Numerical analysis of foundation columns to support widening of embankments", *Comput. Geotech.*, **34**(6), 435-448. https://doi.org/10.1016/j.compgeo.2007.01.006.

Hassen, G., de Buhan, P. and Abdelkrim, M. (2010), "Finite element implementation of a homogenized constitutive law for stone column-reinforced foundation soils, with application to the design of structures", *Comput. Geotech.*, **37**(1-2), 40-49. https://doi.org/10.1016/j.compgeo.2009.07.002.

Hong, Y.S. and Wu, C.S. (2013), "The performance of a sand column internally reinforced with horizontal reinforcement layers", *Geotext. Geomembr.*, **41**, 36-49. https://doi.org/10.1016/j.geotexmem.2013.10.002.

Hosseinpour, I., Riccio, M. and Almeida, M.S. (2014), "Numerical evaluation of a granular column reinforced by geosynthetics using encasement and laminated disks", *Geotext. Geomembr.*, **42**(4), 363-373. https://doi.org/10.1016/j.geotexmem.2014.06.002.

Hughes, J.M.O. and Withers, N.J. (1974), "Reinforcing of soft cohesive soils with stone columns", *Ground Eng.*, **7**(3), 42-49.

Juran, I. and Guermazi, A. (1988), "Settlement response of soft soils reinforced by compacted sand columns", *J. Geotech. Eng.*, **114**(8), 930-943. https://doi.org/10.1061/(ASCE)0733-9410(1988)114:8(930).

Kadhim, S.T., Parsons, R.L. and Han, J. (2018), "Three-dimensional numerical analysis of individual geotextile-encased sand columns with surrounding loose sand", *Geotext. Geomembr.*, **46**(6), 836-847. https://doi.org/10.1016/j.geotexmem.2018.08.002.

Keykhosropur, L., Soroush, A. and Imam, R. (2012), "3D numerical analyses of geosynthetic encased stone columns", *Geotext. Geomembr.*, **35**, 61-68. https://doi.org/10.1016/j.geotexmem.2012.07.005.

Lee, K.Z.Z., Chang, N.Y. and Ko, H.Y. (2010), "Numerical simulation of geosynthetic-reinforced soil walls under seismic shaking", *Geotext. Geomembr.*, **28**(4), 317-334. https://doi.org/10.1016/j.geotexmem.2009.09.008.

Lo, S.R., Zhang, R. and Mak, J. (2010), "Geosynthetic-encased stone columns in soft clay: A numerical study", *Geotext. Geomembr.*, **28**(3), 292-302. https://doi.org/10.1016/j.geotexmem.2009.09.015.

Madhavi, L. and Murthy, V.S. (2007), "Effects of reinforcement form on the behavior of geosynthetic reinforced sand", *Geotext. Geomembr.*, **25**(1), 23-32. https://doi.org/10.1016/j.geotexmem.2006.09.002.

Malarvizhi, S.N. and Ilamparuthi, K. (2007), "Comparative study on the behavior of encased stone column and conventional stone column", *Soils Found*., **47**(5), 873-885. https://doi.org/10.3208/sandf.47.873.

Mazumder, T., Rolaniya, A.K. and Ayothiraman, R. (2018), "Experimental study on behaviour of encased stone column with tyre chips as aggregates", *Geosynth*. *Int*., **25**(3), 259-270. https://doi.org/10.1680/jgein.18.00006.

McGuire, M., Sloan, J. and Filz, G. (2019), "Effectiveness of geosynthetic-reinforcement for load transfer in column-supported embankments", *Geosynth*. *Int*., 1-48. https://doi.org/10.1680/jgein.19.00012.

McKelvey, D., Sivakumar, V., Bell, A. and Graham, J. (2004), "Modelling vibrated stone columns in soft clay", *Proc*. *Inst*. *Civ*. *Eng*. *Geotech*. *Eng*., **157**(3), 137-149.

Miranda, M. and Costa, A.D. (2016), "Laboratory analysis of encased stone columns", *Geotext*. *Geomembr*., **44**(3), 269-277. https://doi.org/10.1016/j.geotexmem.2015.12.001.

Muir Wood, D., Hu, W. and Nash, D.F.T. (2000), "Group effects in stone column foundations: model tests", *Géotechnique*, **50**(6), 689-698. https://doi.org/10.1680/geot.2000.50.6.689.

Najjar, S.S., Sadek, S. and Maakaroun, T. (2010), "Effect of sand columns on the undrained load response of soft clays", *J*. *Geotech*. *Geoenviron*. *Eng*., **136**(9), 1263-1277. https://doi.org/10.1061/(ASCE)GT.1943-5606.0000328.

Nazariafshar, J. and Ghazavi, M. (2014), "Experimental studies on bearing capacity of geosynthetic reinforced stone columns", *Arab*. *J*. *Sci*. *Eng*., **39**(3), 1559-1571. https://doi.org/10.1007/s13369-013-0709-8.

Nguyen, M.D., Yang, K.H., Lee, S.H., Wu, C.S. and Tsai, M.H. (2013), "Behavior of nonwoven-geotextile-reinforced sand and mobilization of reinforcement strain under triaxial compression", *Geosynth*. *Int*., **20**(3), 207-225. http://dx.doi.org/10.1680/gein.13.00012.

Selvakumar, S. and Soundara, B. (2019), "Swelling behaviour of expansive soils with recycled geofoam granules column inclusion", *Geotext*. *Geomembr*., **47**(1), 1-11. https://doi.org/10.1016/j.geotexmem.2018.08.007.

Shahu, J.T. and Reddy, Y.R. (2011), "Clayey soil reinforced with stone column group: model tests and analyses", *J*. *Geotech*. *Geoenviron*. *Eng*., **137**(12), 1265-1274. https://doi.org/10.1061/(ASCE)GT.1943-5606.0000552.

Sivakumar, V., Jeludine, D.K.N.M., Bell, A., Glynn, D.T. and Mackinnon, P. (2011), "The pressure distribution along stone column in soft clay under consolidation and foundation loading", *Géotechnique*, **61**(7), 613-620.

Sivakumar, V., McKelvey, D., Graham, J. and Hughes, D. (2004), "Triaxial tests on model sand columns in clay", *Can*. *Geotech*. *J*., **41**(2), 299-312. https://doi.org/10.1139/t03-097.

Stoeber, J.N. (2012), "Effects of maximum particle size and sample scaling on the mechanical behavior of mine waste rock, a critical state approach", Ph.D. Dissertation, Colorado State University, Fort Collins, Colorado, U.S.A.

Systèmes, D. (2014), Abaqus Version 6.14-2. *User Documentation*.

Tang, L., Cong, S., Ling, X., Lu, J. and Elgamal, A. (2015), "Numerical study on ground improvement for liquefaction mitigation using stone columns encased with geosynthetics", *Geotext*. *Geomembr*., **43**(2), 190-195. https://doi.org/10.1016/j.geotexmem.2014.11.011.

Trautmann, C. H., Kulhawy, F. H., & Longo, V. J. (1987). *CUFAD: A Computer Program for Compression and Uplift Foundaton Analysis and Design* in *Foundation Engineering: Current Principles and Practices*, 691-705.

Vetri Selvan, A. and Raj, D. (2006), "Vibro replacement as foundation for tank farms in India", *Proceedings of the Indian Geotechnical Conference*, Chennai, India, December.

Wu, C.S. and Hong, Y.S. (2008), "The behavior of a laminated reinforced granular column", *Geotext*. *Geomembr*., **26**(4), 302-316. https://doi.org/10.1016/j.geotexmem.2007.12.003.

Wu, C.S. and Hong, Y.S. (2009), "Laboratory tests on geosynthetic-encapsulated sand columns", *Geotext*. *Geomembr*., **27**(2), 107-120. https://doi.org/10.1016/j.geotexmem.2008.09.003.

Xue, J., Liu, Z. and Chen, J. (2019), "Triaxial compressive behaviour of geotextile encased stone columns", *Comput*. *Geotech*., **108**, 53-60. https://doi.org/10.1016/j.compgeo.2018.12.010.

Zhang, L. and Zhao, M. (2014), "Deformation analysis of geotextile-encased stone columns", *Int*. *J*. *Geomech*., **15**(3), 04014053. https://doi.org/10.1061/(ASCE)GM.1943-5622.0000389.

Zhang, L., Zhao, M., Shi, C. and Zhao, H. (2012), "Settlement calculation of composite foundation reinforced with stone columns", *Int*. *J*. *Geomech*., **13**(3), 248-256. https://doi.org/10.1061/(ASCE)GM.1943-5622.0000212.

CC